

# **Assessing the interior structure of the super-Earth exoplanet K2-18b**

MS THESIS

Submitted to

Indian Institute of Science Education and Research, Pune

in partial fulfilment of the requirements for the

BS-MS Dual Degree Programme

by

Daspute Mangesh Pandharinath

20141069

Department of Physics

Indian Institute of Science Education and Research Pune

Dr. Homi Bhabha Road,

Pashan, Pune 411008, India.

March 20, 2018

Supervisors:

Dr Ravi Kumar Kopparapu (NASA Goddard Space Flight Centre, USA)

Dr. Prasad Subramanian (IISER Pune)

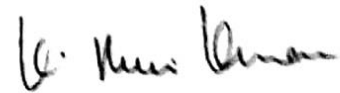
TAC: Suhas Ettamal (IISER Pune)

©Daspute Mangesh Pandharinath 2018

All Rights Reserved

## **Certificate**

This is to certify that this dissertation entitled "Assessing the interior composition of the super-Earth planet K2-18b" towards the partial fulfilment of the BS-MS dual degree programme at the Indian Institute of Science Education and Research, Pune represents study/work carried out by "Daspute Mangesh Pandharinath (IISER Pune)" under the supervision of "Dr. Ravi Kumar Kopparapu, Research Scientist, NASA Goddard Space Flight Center" during the academic year 2018-2019.



Dr. Ravi Kumar Kopparapu

APRIL, 2<sup>nd</sup>, 2019

Supervisors:

Dr. Ravi Kumar Kopparapu

Dr. Prasad Subramanian

TAC:

Dr. Suhas Ettamal



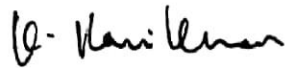
Daspute Mangesh Pandharinath

## Declaration

I hereby declare that the matter embodied in the report entitled "Assessing the interior composition of the super-Earth planet K2-18b" are the results of the work carried out by me at the Department of Physics, IISER Pune, under the supervision of Dr. Ravi Kumar Kopparapu and the same has not been submitted elsewhere for any other degree.



Daspute Mangesh Pandharinath



Dr. Ravi Kumar Kopparapu

APRIL 2<sup>nd</sup> 2019

## **Acknowledgement**

First of all I would like to acknowledge my supervisors Dr. Ravi Kumar Kopparapu, NASA Goddard Space Flight Center and Dr. Prasad Subramanian, IISER Pune for their immense support throughout the project. Without Dr. Kopparapu I would not have been able to explore this field of extrasolar planets. Thanks for the freedom and encouragement he provided. Thanks to Dr. Prasad for making sure that I can do this project remotely. Guidance and support by Dr. Sudha Rajamani and Dr. Suhas Ettamal during my project work is nothing less than a blessing. Also, thanks to IISER for providing such an amazing environment for research.

I would also like to thank Pankaj Bhagwat, Kaarthik Abhinav and Jayanth Kumar and Daniel who have helped me with programming. I thank Harshith Banchimanchi for his idea of doing this project remotely. I would also like to thank my friends a lot who were there to support mentally if I got stuck with some problem. I thank my parents and sister for understanding me and let me pursue my interest in research.

# Contents

<b>Certificate</b> .....	2
<b>Declaration</b> .....	3
<b>Acknowledgement</b> .....	4
<b>List of figures</b> .....	6
<b>List of tables</b> .....	6
<b>Abstract</b> .....	7
<b>1. Introduction</b> .....	8
<b>2. Method and Results</b> .....	9
<b>2.1 Mass-radius curve</b> .....	9
<b>2.2 Ternary diagram</b> .....	11
<b>2.3 Equation of States (EOSs)</b> .....	13
<b>2.4 Bayesian Inference</b> .....	14
<b>3. Discussion and Conclusion</b> .....	19
<b>4. Future Plan</b> .....	20
<b>Bibliography</b> .....	20

## **List of figures**

1. Mass radius curve for planets.....	09
2. Ternary diagram for K2-18 b Cloutier data.....	11
3. Ternary diagram for K2-18 b Sarkis data.....	12
4. Bayesian inference for K2-18 b Cloutier data.....	14
5. Bayesian inference for K2-18 b Sarkis data.....	15

## **List of tables**

1. Measured mass, radius and uncertainty for K2-18 b.....	10
2. Coefficients for EOSs of water-ice, mantle and core.....	12

## **Abstract**

K2-18 b is a super-earth exoplanet revolving around an M-dwarf star K2-18 in constellation Leo. Here we have analysed the internal structure of exoplanet K2-18 b for mass and radius measurement by Cloutier et.al 2017[16] and new combined measurements by Sarkis et. al. 2018[17]. We used Zeng and Seager 2008[1] code to infer range of possible composition of this planet. We present posterior likelihood of core, mantle and water-ice mass fractions of this planet using Bayesian inference.

# 1. Introduction

Exoplanets also known as Extra solar planets are the planets which are not part of our solar system. Some of these extrasolar planets form their solar system with a host star. As on March 27, 2019; 3926 planets have been confirmed. One of the main goals of exoplanet research is to find life on a planet outside our solar system.

M-dwarfs are colder stars than the sun and abundant in our solar neighbourhood. They have effective temperatures between 2500 Kelvin to 4000 Kelvin compared to 5700 Kelvin for the Sun. The habitable zone, which is defined as the region around a star where liquid water can sustain on the surface of a rocky planet, around M-dwarf stars overlaps with tidal locking radius. So exoplanets around M-dwarf stars, which receive stellar radiation comparable to earth, are also affected by the differential gravity of the star. It produces heat at the expense of orbital eccentricity. It also increases plate tectonic activity which drives the Carbonate-Silicate cycle which can stabilise temperature on the surface of a planet. Potentially habitable exoplanets around M-dwarf stars may be in synchronous rotation which can result in one side of the planet always facing the star with perpetual daylight. Remaining part is always the night side. Tidal heating and atmospheric circulation help in making surface temperature homogeneous around the planet.

Super-earths are planets with a mass between 1 to 10 times that of the Earth. These planets could be made of interior ice layers, unlike Earth, and could be scaled up versions of ice-satellites within our solar system like Europa or Ganymede. There is no super-Earth planet in our Solar System. Earth has a very small amount of water(less than one percent) as compared to its total mass. Depending upon the available water content during the formation of the planet, super-earths can have a significant mass of ice or water in them. The interior structure of an exoplanet affects the properties of its surface, atmosphere and habitability. It also determines how it will respond to the differential force of gravity (tidal force) of the host star and neighbouring exoplanets. Using transit and radial velocity techniques, astronomers get to know the mass and radius of exoplanets but knowing their interior structure just with remote observations is not possible. Spectroscopic data of atmosphere or direct image of most of the super-earth exoplanets (including K2-18b) is not available. So observational data of mass and radius is used here to understand the interior and surface properties of exoplanets.

## 2. Method and Results

### 2.1 Mass-radius curve

First, we extracted a list of super-earth exoplanets around M-dwarfs from [NASA Exoplanet Archive](#). We calculated insolation on each of these planets and the equilibrium temperature. We plotted mass-radius curves of the idealised planet (figure 1) with-

1. Rocky interior, ie. 0 % ice by mass (red) and
2. 50% ice/water by mass (blue) as shown in figure 1 using results from C. Sotin et al. 2007[13].

We plotted planets with known mass and radius from the list on the same graph.

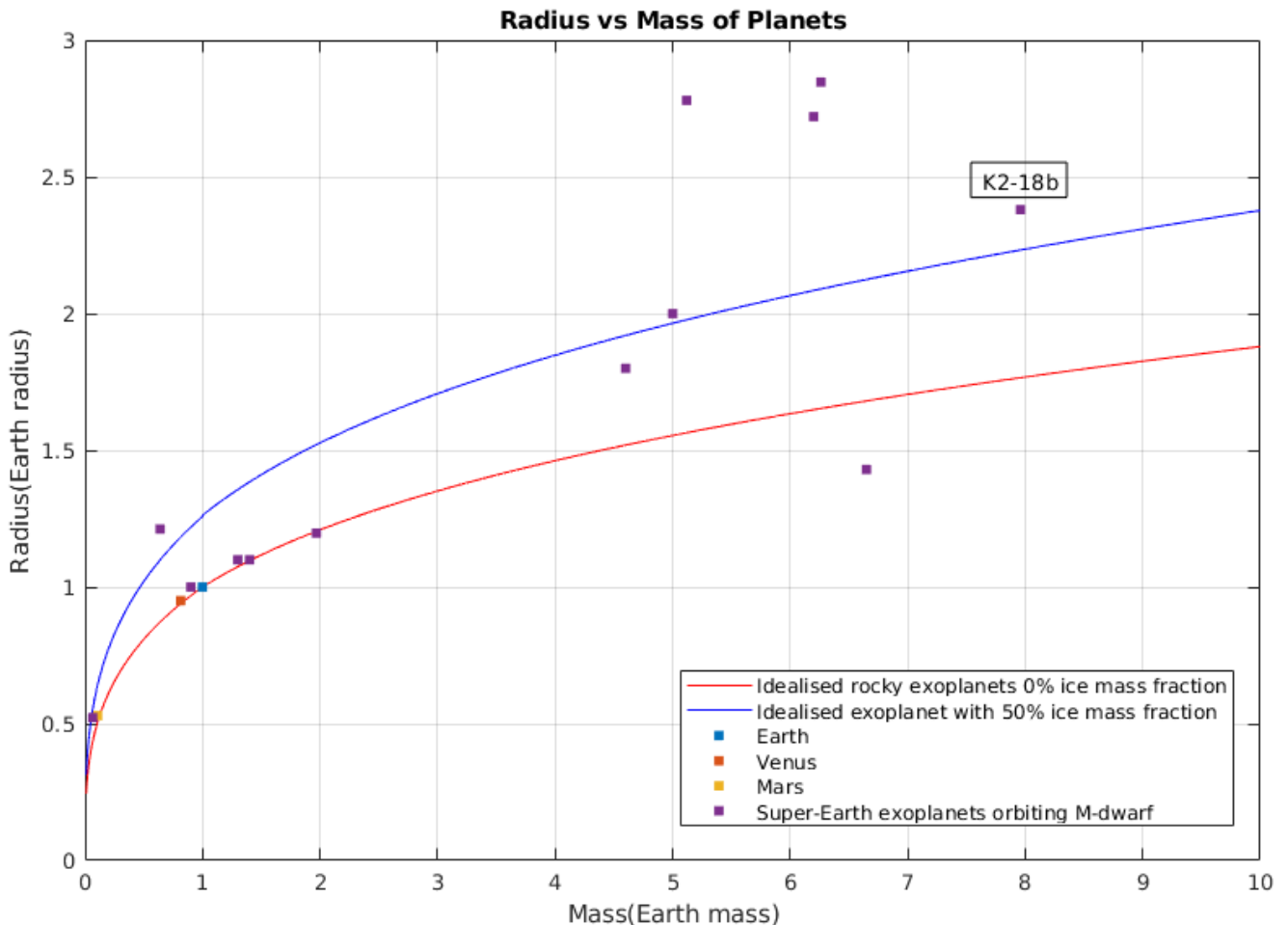


Figure 1: Mass-radius diagram for planets. Earth, Venus and Mars lie on rocky curve. K2-18 b lies above 50% ice mass fraction curve indicating it may have some ice in its interior. Red line represent radius of planet with zero ice mass fraction and Fe/Si abundance ratio as that of Earth. Blue curve represent radius of planet with 50% ice mass fraction.

K2-18b is one of the planets which has insolation 1.06 times that of the Earth allowing it to be in the habitable zone of its host star. The mass and radius of this planet place it close to the 50% ice mass fraction curve, indicating different phases of water could dominate the interior. Its orbital period is 39.2 days, and it is 0.1429AU away from its host star K2-18. It is M2.5 V spectral type star. It is 34pc away from the Earth. All of these things make it an interesting candidate for study. Table 1. Shows measured mass and radius and their uncertainty based on Cloutier et al. 2017[16] and Sarkis et al. 2018[17].

	$M_p$	$\sigma_{M_p}$	Percentage uncertainty	$R_p$	$\sigma_{R_p}$	Percentage uncertainty
Cloutier data[16]	7.96	1.91	23.99%	2.38	0.22	9.24%
Sarkis data[17]	8.92	1.70	19.06%	2.37	0.22	9.28%

*Table 1. Measured mass, radius and their uncertainty for K2-18 b.*

To understand the composition of K2-18b, first, we assumed major components of a differentiated solid exoplanet are- iron core, silicate mantle and a water-ice(ice and ocean layers) outer layer (Figure 2). Mass of gas layer or the atmosphere is insignificant as compared to total mass of the planet for super-earths. So in our study we are considering other three layer.

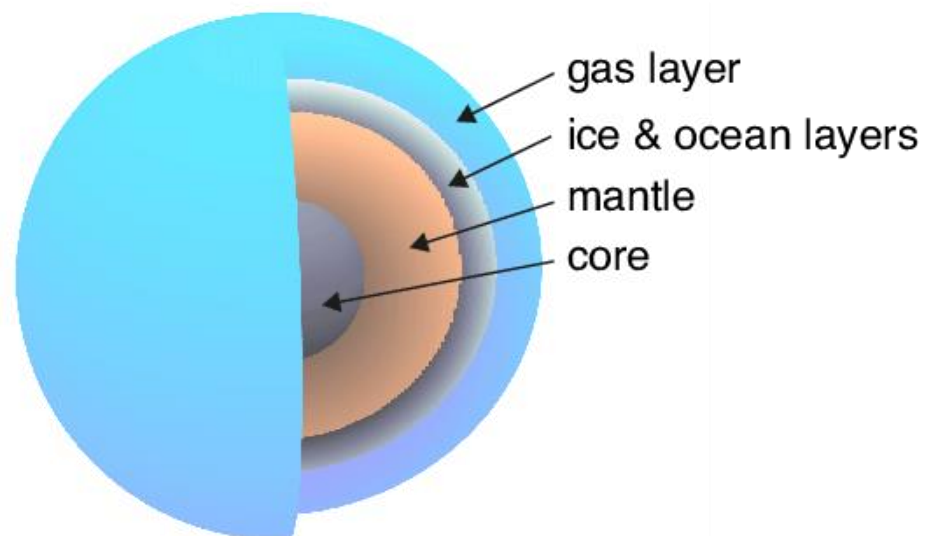


*Figure 2 Internal structure of exoplanet showing different layers. Image source-[10]*

We used publicly available code described in Zeng and Seager (2008) to know what is the mass fractions (MF) of each of these layers. This code considers hydrostatic balance inside exoplanet and equation of state of iron (core), perovskite (mantle), and water-ice VII, VIII and X form of ice at high pressure (water/ice layer). Effect of atmospheric absorption in measured radius is negligible for Super-earth and hence neglected.

## 2.2 Ternary diagram

Using a publically available code by Zeng and Seager, 2008[1], we found that ice mass fraction in K2-18b is around 0.93 to 0.96 and rest is mantle and core (figure 2). Each point on the ternary diagram represents a unique composition. Mass fraction decreases from 1.0 at the apex of the axis to 0.0 at the opposite base. So from bottom to top ice mass fraction increase from 0.0 to 1.0. The blue curve at the top of the attached image represents a possible composition for mass and radius of k2-18b. Green, yellow and red curves represent composition for 1, 2 and 3 standard deviation (in observed data of mass and radius) respectively.

The figure also shows the degeneracy of the problem. We have two constraints the observed mass and observed radius of the planet. Sum of mass fractions of the three components is one is implied from mass being fixed. So it does not count as an independent constraint. Unknown variables are the three Mass fractions water-ice mass fraction (IMF), mantle mass fraction (MMF) and core mass fraction (CMF). The different composition or mass fractions can give the same mass and radius.

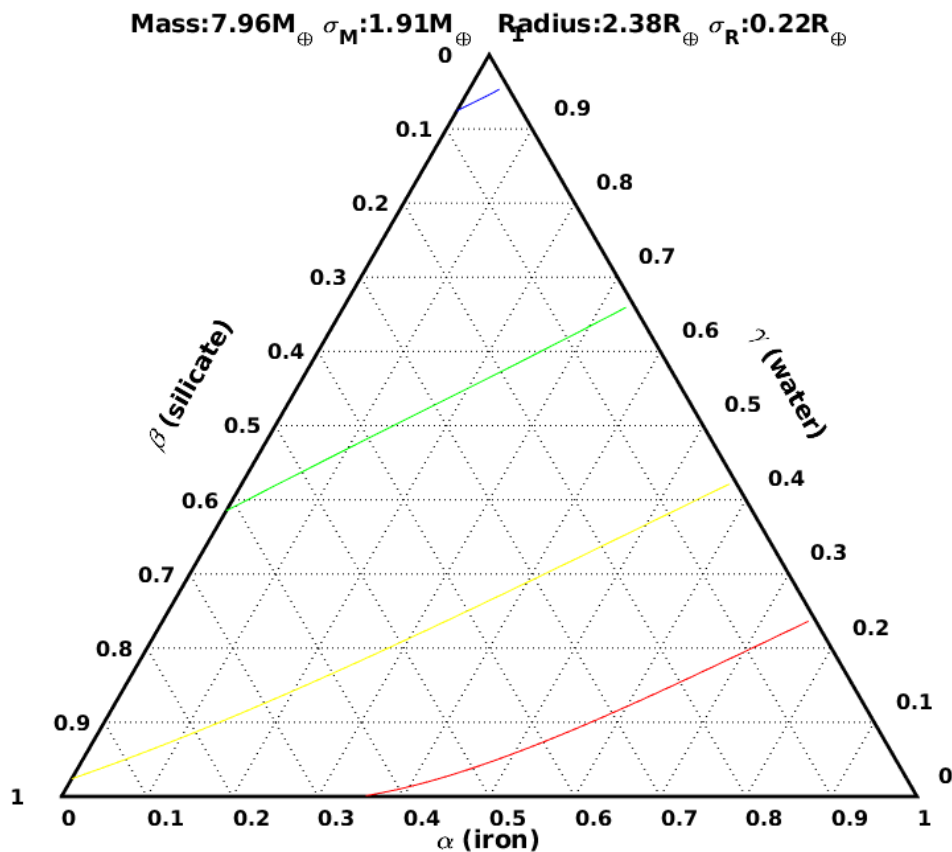


Figure 3: Ternary diagram of K2-18 b composition for Cloutier et.al 2017[16] data implies Ice mass fraction in K2-18b is around 0.93 to 0.96 and rest is mantle and core. Mass fraction decreases from 1.0 at the apex of the axis to 0.0 at the opposite base. So from bottom to top ice mass fraction increase from 0.0 to 1.0. The blue curve at the top of the attached image represents a possible composition for mass and radius of k2-18b. Green, yellow and red curves represent composition for 1, 2 and 3 standard deviation (in observed data of mass and radius) respectively.

Based on Sarkis data, the average density of the planet is 4.11g/cc which is higher than measured for Cloutier data i.e. 3.3g/cc. Because of this, curves on ternary (figure 3) diagram shift to lower value of least dense material i.e. towards low IMF. It spans from 0.76 to 0.86.

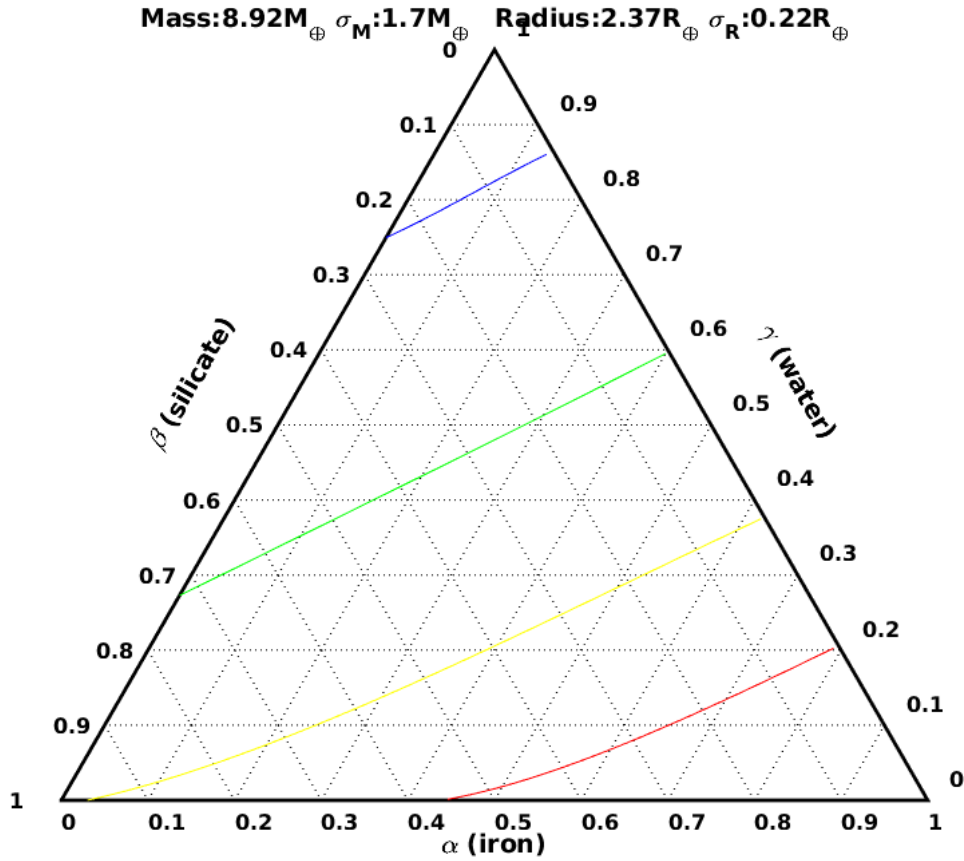


Figure 4 Ternary diagram of K2-18 b composition for Sarkis data implies Ice mass fraction in K2-18b is spans from 0.76 to 0.86 and rest is mantle and core. Mass fraction decreases from 1.0 at the apex of the axis to 0.0 at the opposite base. So from bottom to top ice mass fraction increase from 0.0 to 1.0. The blue curve at the top of the attached image represents a possible composition for mass and radius of k2-18b. Green, yellow and red curves represent composition for 1, 2 and 3 standard deviation (in observed data of mass and radius) respectively.

### 2.3 Equation of States (EOSs)

Equation of states used in this work is approximate EOS which is modified polytropic EOS described in Seager et al. 2007. This EOS relates pressure and density of a material and is of the form  $\rho(P) = \rho_0 + cP^n$  where  $\rho_0$  is density at zero pressure, c and n are constants depending on the material.

Material	$\rho_0$ (kg m <sup>-3</sup> )	c (kg m <sup>-3</sup> Pa <sup>-n</sup> )	n
Fe( $\alpha$ )	8300.00	0.00349	0.528
MgSiO <sub>3</sub> (perovskite)	4100.00	0.00161	0.541
High pressure H <sub>2</sub> O	1460.00	0.00311	0.513

Table 2. Coefficients for approximate EOS

To describe the relationship between pressure and density at 300° K, Vinet or Birch-Murnaghan EOS is appropriate for low pressure (typically <200GPa) and fits with experimental data, and Thomas-Fermi-Dirac EOS is appropriate for high pressure (typically above 10<sup>4</sup> GPa). The approximate EOS fits with experimental data at low pressure and shifts to Thomas-Fermi-Dirac EOS at higher pressure. Effect of temperature on the density of the material and hence the radius of a solid planet is very little, and so it is neglected in approximate EOS.

## 2.4 Bayesian Inference

Ternary diagram show a range of possible compositions for the interior of exoplanets for given mass, radius and their observational uncertainties. But since more than one model parameter is uncertain and different combinations of model parameters can give same mass and radius of the planet, no bounds on ternary diagrams do not represent quantitative likelihood or probability of the composition. Bayesian inference considers this and provides the posterior likelihood to every parameter (e.g. core mass fraction (CMF), mantle mass fraction (MMF) and mass of the planet (M<sub>p</sub>)). IMF is not explicitly used as a parameter because of the constrain 1=CMF+MMF+IMF because of a fixed mass of the planet. We are considering flat prior for IMF, MMF and CMF. Bayesian inference used in this study is based on Roger and Seager 2010 [5].

Likelihood function[5] for this Bayesian analysis is given by-

$$L(M_p, CMF, MMF) = \frac{e^{-\frac{(M_p - \widehat{M}_p)^2}{2\sigma_{M_p}^2}} - \frac{(R_p - \widehat{R}_p)^2}{2\sigma_{R_p}^2}}{2\pi\sigma_{M_p}\sigma_{R_p}}$$

Where  $\hat{M}$  is used to represent the mass of the planet as a parameter and calculated radius of the planet.

Markov Chain Monte Carlo method is used for sampling compositions. Metropolis algorithm is used for iterations. Proposed composition (a set of the model parameter) is accepted with probability  $P_{\text{accept}}$  explained in Mosegaard & Tarantola 1995[19].

$$P_{\text{accept}} = \min\{1, \exp(\ln(\text{proposed composition} | \text{data}) - \ln(\text{old composition} | \text{data}))\}$$

For Cloutier and Sarkis data sets, 1110000 samples of composition were generated of which initial 10000 were rejected. Effect of atmospheric pressure on the internal structure of the planet is neglected. Figure 3 and Figure 4 show results for Bayesian inference for K2-18 b for Cloutier and Sarkis data respectively. The graphs show the posterior likelihood of CMF, IMF and MMF. From both the graphs, it is clear that the planets will have a large amount of high-pressure Ice. CMF and IMF are more likely to be small. So it looks like scaled up versions of ice-satellites within our solar system.

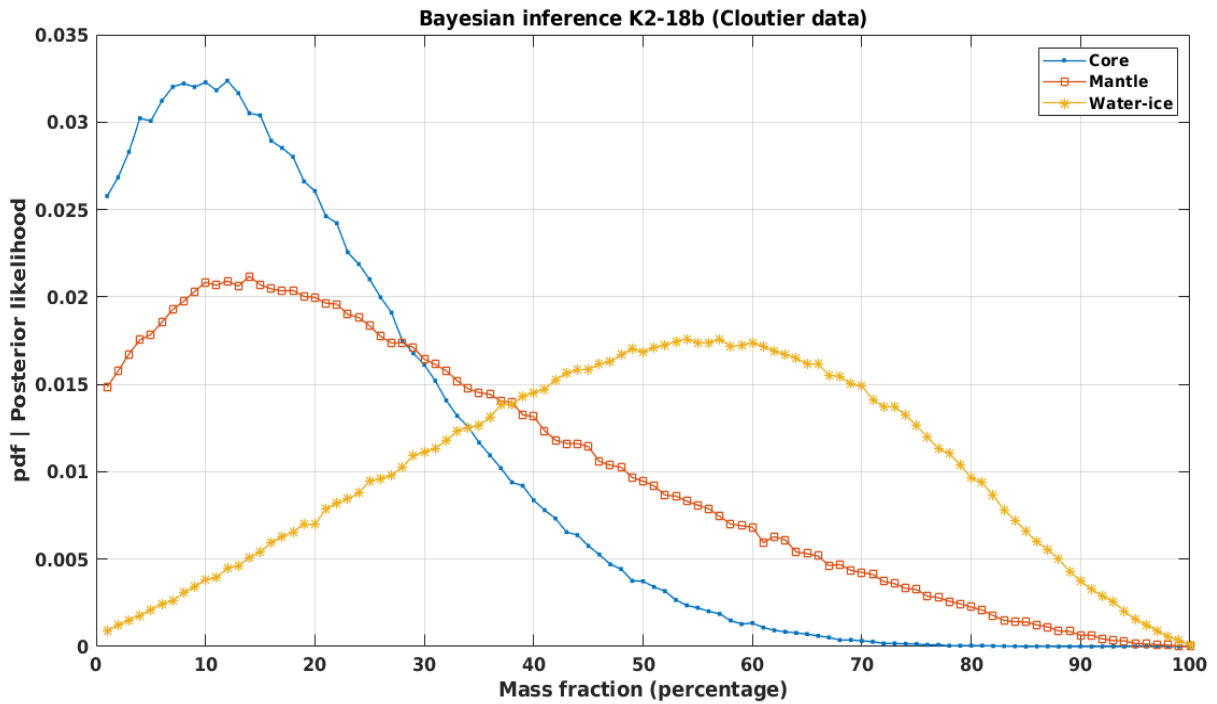


Figure 5.- Bayesian inference results- Posterior likelihood of CMF, MMF and IMF of K2-18 b for Cloutier et.al.2017[16] data. X-axis represents percentage mass fraction and y-axis represent probability.

Peaks in the posterior likelihood of IMF, CMF and MMF are not sharp because of

1. Large uncertainty in observed mass and radius of K2-18 b for both Sarkis and Cloutier data.
2. Inherent degeneracy of the problem.

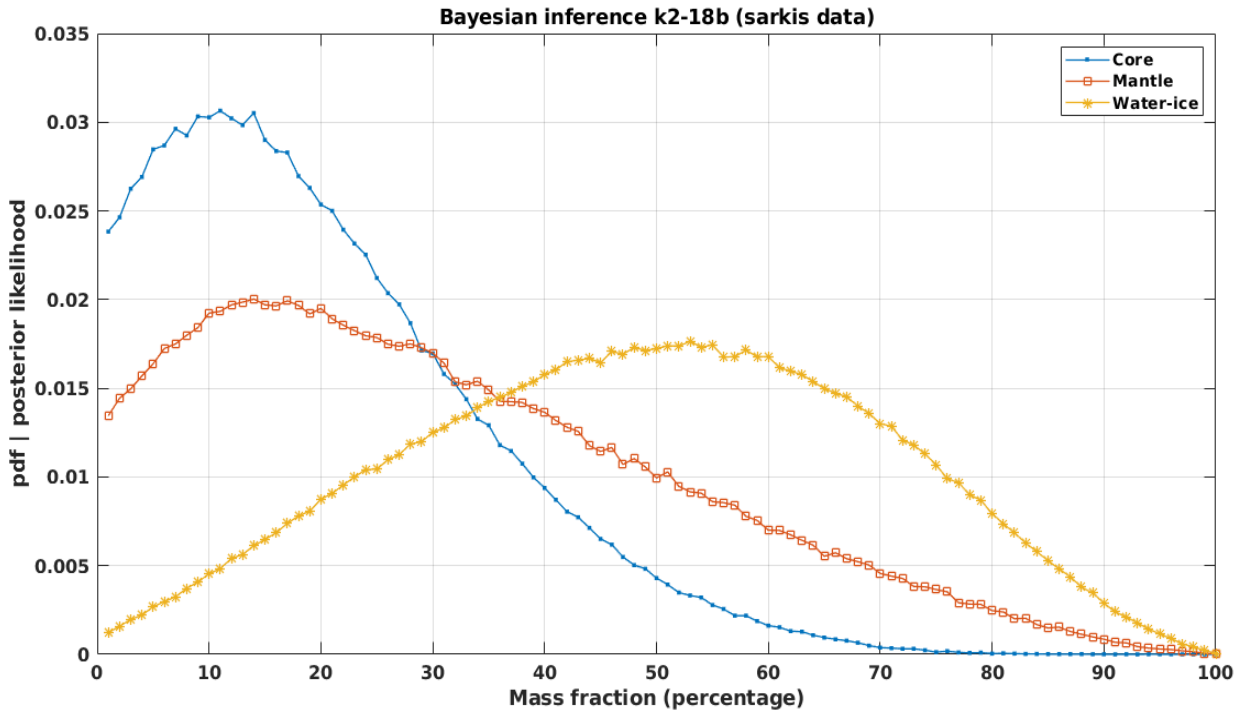


Figure 6.- Bayesian inference results- Posterior likelihood of CMF, MMF and IMF of K2-18 b for Sarkis data.

Peaks for core and mantle mass fractions for data by Serkis is lesser than that for Cloutier. These curves are also shifted to higher mass fractions. Implying core and mantle mass fractions is more than what is calculated from Cloutier data. The curve for the water-ice mass fraction is shifted to left.

Figure 4 represents the inferred structure of selected moons of Saturn and Jupiter[21].

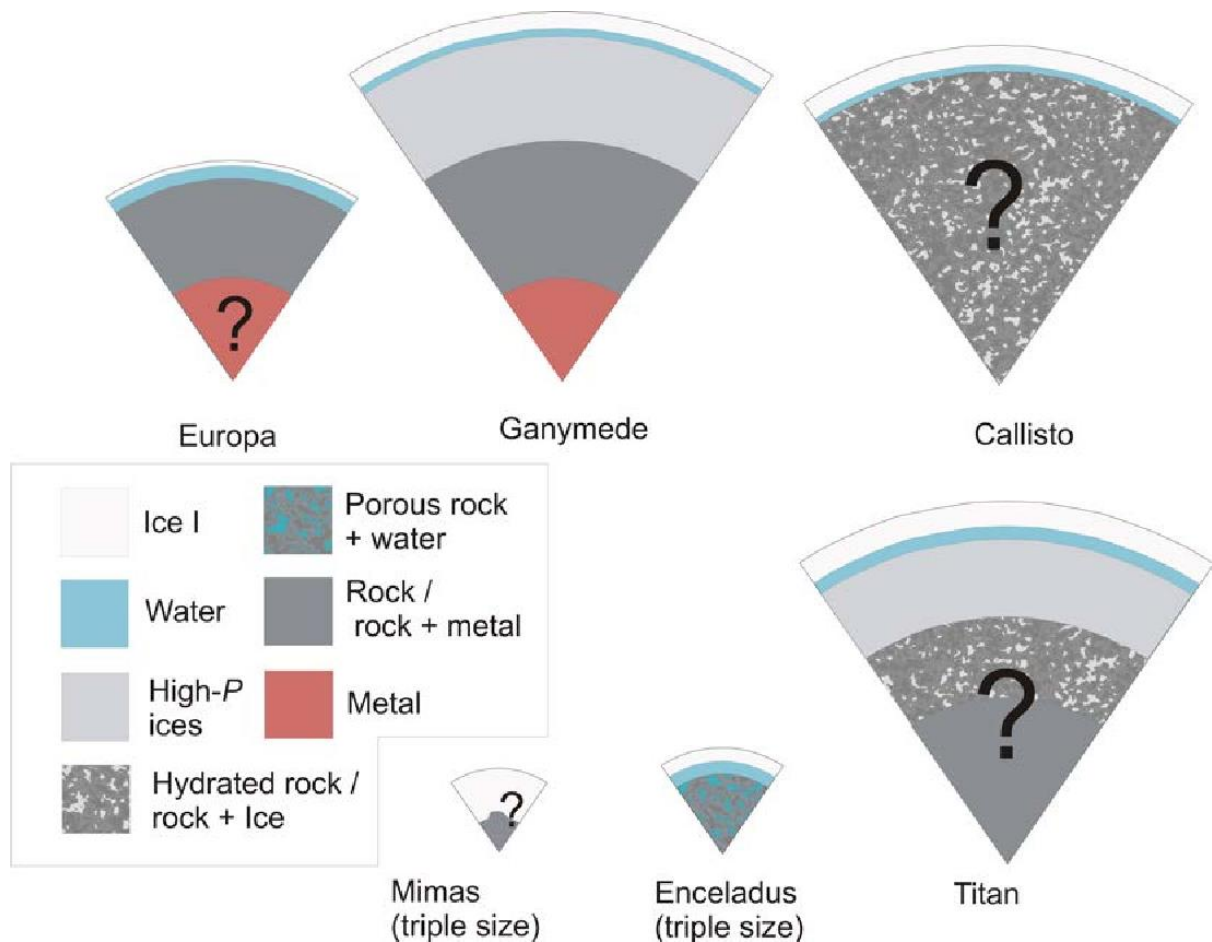


Figure 7 Inferred internal structures for selected moons of Jupiter and Saturn. Question marks indicate regions of particular uncertainty. Mimas and Enceladus are plotted at three times the scale of the other moons[21].

If we consider the internal structure of K2-18 b for the peak of each curve in Bayesian inference, mass fractions roughly resembles that of Ganymede. Thus the internal structure of K2-18 b can be considered as scaled up vision of Ganymede. Stellar flux for K2-18 b planet is  $1437\text{W/m}^2$  compared to Earth( $1361\text{W/m}^2$ ), Venus( $2601\text{W/m}^2$ ) and Mars( $586\text{W/m}^2$ ). Bayesian inference indicate that there is a high probability that the IMF is non-zero, implies surface will be covered with water or ice, and this planet can have a water vapour atmosphere.

### **3. Discussion and Conclusion**

This kind of analysis can be easily extended to other exoplanets like Kepler-26 c, LHS-1140 b which are super-earths revolving around M-dwarf stars in the habitable zone.

Radius and Mass measurement data used here had a standard deviation (figure 1). More precise measurements of mass and radius are required for getting more informative results.

Since the problem of finding the interior structure of exoplanet is underconstrained, more number of constraints are required to determine the internal structure of the planet precisely. For eg. Measurement of magnetic field and rotation rate of exoplanets can put a constraint on size and mass fraction of core[18]. For habitable planets around M-dwarf stars like K2-18 b, which are in synchronous rotation, rotational rate and revolution rate are usually the same. So measurement of the magnetic field of the planet will improve estimates of its interior structure.

If observed radius of the planet is higher than the actual radius of solid planet due to atmospheric absorption then this analysis need to be improved by either considering atmosphere as a forth layer, which will increase degeneracy further, or by estimating how many fractions of radius is due to atmospheric absorption using a parameter for optical depth or number of opaque scale hights, then correcting for radius for solid planet and analysing using Bayesian inference for three layers.

## 4. Future Plan

We are estimating numerical difference between transit radius and solid surface of the planet[20] and pressure exerted by the atmosphere on the surface of the planet[5]. We are going to study the effect of tidal heating due to host star K2-18 and another exoplanet of same solar system K2-18 c using n-body integrator called Posidonius (Blanco-Cuaresma & Bolmont, 2017[2]).

## Bibliography

Reference 1 to 18 are part of reading for this project.

- 1) Zing and Seager *A computational tool to interpret the bulk composition of solid exoplanets based on mass and radius measurements*, Astronomical society of Pacific, 120:983–991, 2008
- 2) Sergi Blanco-Cuaresma and Emeline Bolmont *Studying tidal effects in planetary systems with Posidonius. A N-body simulator written in Rust*, Zenodo, 2017
- 3) Dorn et al. *A generalised Bayesian inference method for constraining the interiors of super-Earths and sub-Neptunes*, A&A, 597, A37, 2017
- 4) Dorn et al. *Can we constrain interior structure of rocky exoplanets from mass and radius measurements?*, A&A, 577, A83, 2015
- 5) Rogers and Seager, *A framework for quantifying the degeneracy of exoplanet interior composition*, The Astrophysical Journal, 712, 974–991, 2010 April 1
- 6) Valencia et al. *Detailed model of super-Earths: How well can we infer bulk properties?* The Astrophysical Journal, 665, 1413–1420, 2007 August 20
- 7) Valencia et al. , *Internal structure of massive terrestrial planets*, 181, 2, 545-554, April 2006
- 8) Brian Jackson, Rory Barnes and Richard Greenburg, *Tidal heating of terrestrial extrasolar planets and implications for their habitability*, 391, 1, 21, 237–245, November 2008

- 9) Spiegel et al. , *The structure of exoplanets*, PNAS 111 (35) 12622-12627, September 2, 2014
- 10) Caroline Dorn, Dan J. Bower, Antoine Rozel, *Assessing the interior structure of terrestrial exoplanets with implications for habitability*, Springerlink, 3111-3135, 03 November 2018
- 11) J.E. Chambers, *A hybrid symplectic integrator that permits close encounters between massive bodies*, Monthly Notices of the Royal Astronomical Society, 304, 4, 793–799, 16 April 1999
- 12) Bolmont et al. *Mercury-T: A new code to study tidally evolving multiplanet systems. Applications to Kepler-62*, A&A, 583, A116, 2015
- 13) Sotin et al. *Mass-radius curve for extrasolar Earth-like planets and ocean planets*, 191, 1, 337-351, 1 November 2007
- 14) Henning et al. *Tidally heated terrestrial exoplanets: Viscoelastic response model*, *The Astrophysical Journal*, 707:1000–1015, 2009 December 20
- 15) Rory Barnes, *Tidal locking of habitable exoplanets*, Volume 129,4,509–536, December 2017
- 16) Cloutier et. al. *Characterization of the K2-18 multi-planetary system with HARPS*, A&A, 608, A35, 2017
- 17) Sarkis et al. *The CARMENES search for exoplanets around M-dwarfs: A low-mass planet in the temperate zone of the nearby K2-18*, *The Astronomical Journal*, 155,6, 2018 May 31
- 18) Mercedes López-Morales Natalia Gómez-Pérez, Thomas Ruedas, *Magnetic Fields in Earth-like Exoplanets and Implications for Habitability around M-dwarfs*, NCBI 41(6),533-7, 2011 December
- 19) Mosegaard, K., & Tarantola, A. 1995, J. Geophys. Res., *Monte Carlo sampling of solutions to inverse problems*, *Journal of Geophysical Research* Vol. 100, No., B7, p 12,431–12,447, 1995
- 20) Brad Hansen, *On the absorption and redistribution of energy in IR radiated planets* *The astrophysical journal* 179, 484-508, 2008

21) Francis Nimmo, *Icy Satellites: Interior Structure, Dynamics, and Evolution*, Oxford  
Research encyclopedia of Planetary Science, June 2018